ehp ENVIRONMENTAL HEALTH PERSPECTIVES
http://www.ehponline.org

Novel Roles for Notch3 and Notch4 Receptors in Gene Expression and Susceptibility to Ozone-Induced Lung Inflammation in Mice

Kirsten C. Verhein, Zachary McCaw, Wesley Gladwell, Shweta Trivedi, Pierre R. Bushel, and Steven R. Kleeberger

http://dx.doi.org/10.1289/ehp.1408852

Received: 20 June 2014
Accepted: 5 February 2015
Advance Publication: 6 February 2015

Novel Roles for Notch3 and Notch4 Receptors in Gene Expression and Susceptibility to Ozone-Induced Lung Inflammation in Mice

Kirsten C. Verhein,[1] Zachary McCaw,[1] Wesley Gladwell,[1] Shweta Trivedi,[2] Pierre R. Bushel,[3] and Steven R. Kleeberger[1]

[1]Laboratory of Respiratory Biology, National Institute of Environmental Health Sciences, National Institutes of Health (NIH), Department of Health and Human Resources (DHHS), Research Triangle Park, North Carolina, USA; [2]Department of Animal Science, North Carolina State University, Raleigh, North Carolina, USA; [3]Biostatistics Branch, National Institute of Environmental Health Sciences, NIH, DHHS, Research Triangle Park, North Carolina, USA

Address correspondence to Kirsten C. Verhein, Laboratory of Respiratory Biology, National Institute of Environmental Health Sciences, 111 T.W. Alexander Drive, Building 101, MD D-201, Research Triangle Park, NC 27709. Telephone: 919-316-4673. E-mail: kirsten.verhein@nih.gov

Running title: Notch receptors and ozone-induced inflammation

Acknowledgments: We thank the NIEHS Microarray Core (Dr. Kevin Gerrish, Mr. Rick Fannin, and Ms. Laura Wharey), the NIEHS Histology Core, Dr. Gordon Flake for assistance with lung pathology, and Dr. Jason Williams of the NIEHS Mass Spectrometry Group. We thank Alion Science and Technology for performing ozone exposures. We also thank Drs. Donald Cook and Michael Fessler for critical review of the manuscript. Research was supported by the Intramural Research Program of NIEHS, National Institutes of Health (NIH), and Department of Health and Human Services.

Competing financial interests: The authors have declared no conflict of interest exists.

Abstract

Background: Ozone is a highly toxic air pollutant and global health concern. Mechanisms of genetic susceptibility to ozone-induced lung inflammation are not completely understood. We hypothesized *Notch3* and *Notch4* are important determinants of susceptibility to ozone-induced lung inflammation.

Methods: Wild type (WT), *Notch3* (*Notch3*$^{-/-}$) and *Notch4* (*Notch4*$^{-/-}$) knockout mice were exposed to ozone (0.3 ppm) or filtered air for 6-72 hours.

Results: Relative to air-exposed controls, ozone increased bronchoalveolar lavage fluid (BALF) protein, a marker of lung permeability, in all genotypes, but significantly greater concentrations were found in *Notch4*$^{-/-}$ compared to WT and *Notch3*$^{-/-}$. Significantly greater mean numbers of BALF neutrophils were found in *Notch3*$^{-/-}$ and *Notch4*$^{-/-}$ mice compared to WT mice after ozone. Expression of whole lung *Tnf* was significantly increased after ozone in *Notch3*$^{-/-}$ and *Notch4*$^{-/-}$ mice, and was significantly greater in *Notch3*$^{-/-}$ mice compared to WT. Statistical analyses of the transcriptome identified differentially expressed gene networks between WT and knockout mice basally and after ozone, and included *Trim30*, a member of the inflammasome pathway, and *Traf6*, an inflammatory signaling member.

Conclusions: These novel findings are consistent with *Notch3* and *Notch4* as susceptibility genes for ozone-induced lung injury, and suggest that Notch receptors protect against innate immune inflammation.

Introduction

Ozone is a global, highly toxic air pollutant and principal component of smog. Elevated ambient ozone is associated with increased hospitalizations and exacerbation of respiratory conditions (Bell et al. 2004; Tatum and Shapiro 2005). Numerous components of the innate immune response are altered as a result of ozone toxicity in human and rodent airways including predominant neutrophilic inflammation and airway hyperresponsiveness, chemokine and cytokine production, damage to airway epithelium, and increased mucus production and secretion (Al-Hegelan et al. 2011; Hollingsworth et al. 2007; Oakes et al. 2013). Ozone interacts initially with airway epithelial cells, alveolar macrophages, and epithelial lining fluid to initiate induction of cytokines and chemokines (including TNF, IL-6, IL-8, IL-1β, prostaglandins, GM-CSF) that recruit innate immune cells such as neutrophils. Inter-individual [e.g. (Alexeeff et al. 2008; Chen et al. 2007; McDonnell 1991; Yang et al. 2008)] and inter-strain [e.g. (Bauer et al. 2010; Hamade et al. 2010; Kleeberger et al. 1997; Prows et al. 1997; Vancza et al. 2009)] variation in lung responses to ozone have been reported, but mechanisms of susceptibility are not completely understood.

We used positional cloning to identify candidate ozone-susceptibility genes in a significant quantitative trait locus (QTL) on mouse chromosome 17 (*Inf2*) (Bauer et al. 2010; Kleeberger et al. 1997), including histocompatibility genes and tumor necrosis factor alpha (*Tnf*) which are involved in innate immune function. TNF-α is a key inflammatory cytokine that contributes to ozone-induced pulmonary inflammation (Cho et al. 2007). In humans, an activating polymorphism in *Tnf* enhances susceptibility to ozone and asthma (Lee et al. 2009). Another candidate susceptibility gene in *Inf2* is *Notch4*, and just proximal to *Inf2* is *Notch3*. Notch receptors are evolutionarily conserved cell surface receptors important for cell fate decisions and

embryonic development (Osborne and Minter 2007). In the lung, Notch4 is primarily expressed by endothelial cells, and Notch3 is expressed throughout (Post et al. 2000). Recent evidence suggests Notch signaling is important in a mouse model of allergic asthma. Expression of Notch ligand Jagged1 on dendritic cells is induced by lipopolysaccharide (LPS) and is important for development of allergen-induced airway inflammation (Okamoto et al. 2012). Kang and colleagues inhibited Notch signaling with a γ-secretase inhibitor, which prevented antigen-induced airway inflammation in mice (Kang et al. 2009). In the present investigation, we hypothesized that Notch3 and Notch 4 receptors are critical to lung innate immune inflammatory response to ozone, and in particular the neutrophilic influx into the lung.

Methods

Animals and inhalation exposure

Male *Notch3*$^{-/-}$ (B6;129S1-*Notch3*^{tm1Grid}/J), *Notch4*$^{-/-}$ (B6;129S1-*Notch4*^{tm1Grid}/J) and WT mice (B6129SF1/J) (7-13 wk; average body weight 22.6 g ± 0.3) were purchased from Jackson Laboratories. Males were chosen for this study because we used males in our previous study to identify the *Inf2* QTL on chromosome 17 and we wished to avoid potential confounders such as gender in the present study (Bauer et al. 2010; Kleeberger et al. 1997). Experimental groups had between 3 and 10 mice per group (further details for individual experiments are included in the figure legends). Mice were at the exposure facility for approximately one week before they were acclimated for 2-4 days in individual stainless-steel wire cages in a Hazelton 1000 exposure chamber (Lab Products) containing a charcoal and high-efficiency particulate air-filtered air supply. Mice had access to food and water *ad libitum* (NIH-07 chow, Zeigler Brothers). Mice were exposed continuously to 0.3 ppm ozone for 6, 24, 48, or 72 hours as previously described (Cho et al. 2007) and parallel exposures to filtered air were done in a separate chamber for the

same duration. Ozone was generated with a silent arc discharge ozone generator (model L-11; Pacific Ozone Technology) using ultra-high-purity air (National Welders, Inc.). Chamber air temperature (72 ± 3° F) and humidity (50 ± 15%) were held constant. Ozone concentration was monitored and varied less than 1% over the duration of exposure (Dasibi model 1008-PC; Dasibi Environmental Corp.). Animals were treated humanely and with regard to alleviation of suffering. All animal use was approved by the National Institute of Environmental Health Sciences Animal Care and Use Committee.

Etanercept treatment

Mice were treated with etanercept (Enbrel, 10 mg/kg, i.p., Immunex) or vehicle (human IgG, 10 mg/kg, Abcam) 18 hours before exposure to 0.3 ppm ozone for 24 hours (Budinger et al. 2011). The dose of etanercept was chosen to ensure inhibition of Tnf signaling in the mice for the duration of the ozone exposure (Budinger et al. 2011). Drugs were diluted in sterile phosphate buffered saline (PBS).

Phenotype analysis

Immediately following exposures, animals were killed with sodium pentobarbital (104 mg/kg, i.p.). The right lungs only were lavaged four times with Hanks' balanced salt solution (17.5 ml/kg, pH 7.2-7.4). Lavage fluid was centrifuged and supernatant from the first lavage was assayed for total protein concentration (a marker of lung permeability) using the Bradford assay (Thermo Scientific). Cell pellets were pooled, resuspended in Hanks' balanced salt solution, and counted with a hemocytometer. Cells were spun onto glass slides and stained with Wright-Giesma stain (Diff-Quick, Baxter Scientific Products) for differential cell count analysis.

Nuclear protein extraction and NFκB activation

Nuclear protein was isolated from frozen left lung homogenates using a nuclear extract kit according to manufacturers instructions (Active Motif). Protein concentration was measured using the *DC* protein assay (Bio-Rad Laboratories) and nuclear protein from 3 animals per genotype/exposure group (air, 24 and 48 hours ozone exposure) was equally pooled to achieve 10ug of nuclear protein per NFκB assay well. NFκB activation was measured using a p65 transcription factor assay kit (TransAM p65, Active Motif). Samples were measured in duplicate and the assay was repeated three times.

Total lung RNA isolation and qRT-PCR

Total RNA was isolated from frozen left lung homogenates using the RNeasy Mini Plus Kit (Qiagen) following manufacturer's instructions. One microgram of RNA was reverse transcribed into cDNA using MuLV reverse transcriptase (Life Technologies) at 42° C for 15 minutes and 95° C for 5 minutes with a Gene Amp PCR system 9700 (Applied Biosystems). Real-time qPCR was performed on a 1 μl sample of cDNA with either TaqMan probes or SybrGreen (Life Technologies) using a StepOnePlus Real-Time PCR System (Applied Biosystems, Life Technologies) Taqman Probes: *β-actin* Mm00607939_s1; *Tnf* Mm00443260_g1; *Notch1* Mm00435249_m1; *Notch2* Mm00803077_m1; *Notch3* Mm00435270_m1; *Jag1* Mm00496902_m1; *Jag2* Mm01325629_m1; *Dll1* Mm01279269_m1; *Hes1* Mm01342805_m1; *Cxcl2* Mm00436450_m1. Primers for *Notch4* were: forward-GGA GAC TGC AGA CCA GAA GG, reverse-GAC CCT CAG AGT CAG GGA CA. Quantification of amplified products was performed using the delta-delta-Ct method with β-actin as the internal control.

Microarray analysis of lung transcriptome

Total whole lung RNA was used after passing quality control using an Agilent Bioanalyzer 2100 (Agilent Technologies, Inc.). GeneChip analysis (Affymetrix) on the Affymetrix Mouse Genome 430 2.0 array containing over 39,000 transcripts was performed on each treatment group in triplicate. Expression intensity values were normalized with the Robust Multiarray Average (RMA) method using GeneSpring (GeneSpring GX 11.0 Expression Analysis Software, Agilent Technologies). Transcripts were further analyzed by two-way ANOVA with Tukey's honest significant difference (HSD) post-hoc tests comparing genotype (WT, *Notch3*$^{-/-}$, *Notch4*$^{-/-}$) and exposure (air, 6 hours ozone, 24 hours ozone, 48 hours ozone). Genes were determined to be statistically differentially expressed at the Benjamini-Hochberg multiple testing correction adjusted p-value < 0.05. Gene lists were analyzed using QIAGEN's Ingenuity Pathway Analysis (IPA, QIAGEN Redwood City, http://www.qiagen.com/ingenuity). Microarray data were submitted to CEBS: 005-00003-0112-000-3 and GEO: GSE58244.

EPIG pattern analysis

We also used EPIG (Extracting microarray gene expression Patterns and Identifying co-expressed Genes) to characterize gene expression patterns (Chou et al. 2007). The approach utilizes the underlying structure of gene expression data to extract patterns and identify co-expressed genes that are responsive to experimental conditions. For each genotype group, the RMA normalized data for each probeset was converted to a ratio value by dividing the probeset pixel intensity by the average of its respective time-matched air control samples from that group and then log base 2 transforming the ratio. EPIG uses Pearson correlation (*r*) across all the 9 groups of samples, signal to noise (s/n) ratio within groups of samples, and magnitude of fold change (FC) for a probeset within a group to first detect all potential patterns in the data and co-

expressed gene probesets detected in terms of statistically significant (p-value < 10^{-4}) correlation between the probesets profiles and the pattern. The parameter settings for the EPIG analysis were the defaults: r = 0.8, s/n = 2.5 and FC = 0.5. We used a minimum pattern cluster size of 6 for finding all potential patterns.

Statistics

All data are expressed as group mean ± SE. Two-way ANOVA was used to evaluate effects of ozone on pulmonary injury in WT and knockout mice. Factors in this analysis were exposure (air or ozone) and genotype (wild type, *Notch3*$^{-/-}$, or *Notch4*$^{-/-}$). Data from air-exposed mice were pooled since there was no post-exposure time effect on BALF protein concentration or cells. All statistical analyses were performed with GraphPad Prism (version 6.0, GraphPad Software).

Results and Discussion

Targeted deletion of Notch3 and Notch4 enhances susceptibility to ozone-induced lung inflammation

To assess the role of *Notch3* and *Notch4* in ozone-induced lung inflammation, we exposed continuously to ozone WT mice and mice with targeted deletion of *Notch3* (*Notch3*$^{-/-}$) or *Notch4* (*Notch4*$^{-/-}$) and measured markers of lung inflammation and injury. In mice, sub-acute exposure to 0.3 ppm ozone represents an environmentally relevant dosing protocol that elicits airway inflammation others and we have used previously (e.g. Backus et al. 2010; Cho et al. 2007; Johansson et al. 2010; Kasahara et al. 2012). This dosing protocol was chosen for the current study because it led to the initial discovery of the *Inf2* QTL containing ozone susceptibility genes in mice (Bauer and Kleeberger 2010; Kleeberger et al. 1997).

Although significantly increased compared to air controls, inflammation parameters [bronchoalveolar lavage fluid (BALF) protein and total cells] in WT mice were minimal following ozone exposure (Figure 1A and 1B) compared to more susceptible strains (Cho et al. 2001). Relative to air-exposed controls, deletion of either *Notch3* or *Notch4* markedly enhanced ozone-induced increases in the numbers of macrophages and monocytes in BALF (Figure 1D and 1E and Supplemental Material Table S1) and whole lung expression of proinflammatory mediators *Tnf* and *Cxcl2* (macrophage inflammatory protein 2-alpha, *Mip2*) (Figure 1H and 1I). Lymphocytes in BALF were not consistently changed by ozone exposure; a significant increase was found only after 24 hours ozone in wild type mice (Figure 1G). We also measured an increase in NF-κB activation after 48 hours ozone in *Notch4*$^{-/-}$ mice (Figure 1J). Neither *Notch3* nor *Notch4* were expressed in their respective deletion animals (Figure 2C and 2D) and we found no ozone or genotype effect on known Notch ligands (*Jagged1*, *Jagged2*, and *Dll1*) or the effector molecule *Hes1* (Figure 2E-H).

The most notable change in BALF inflammatory markers was found for neutrophils. Highly significant increases were found in *Notch3*$^{-/-}$ and *Notch4*$^{-/-}$ mice compared to respective air controls and WT (Figure 1C). Moreover, ozone-induced changes in BALF protein, a marker for lung injury, were significantly increased in *Notch4*$^{-/-}$ mice relative to the other genotypes (Figure 1A). These results suggest a protective role for *Notch* in ozone-induced lung injury and inflammation.

A potential mechanism through which Notch3 and Notch4 protect against ozone-induced inflammation is by modulation of *Tnf* expression. TNF-α is increased during ozone-induced airway inflammation and TNF inhibition reduces neutrophilia (Cho et al. 2001; Shore et al. 2001). To determine whether TNF-α mediates exacerbated inflammation in *Notch* deficient

mice, we treated WT, *Notch3*$^{-/-}$ and *Notch4*$^{-/-}$ mice with the TNF-α inhibitor etanercept before ozone exposure. Etanercept had no effect on BALF protein concentration (Figure 3A) as predicted since antibodies to TNF, as well as targeted deletion of TNF receptors and *Tnf* also had no effect on lung permeability (Cho et al. 2001). In wild type mice neutrophils were significantly increased in BALF after ozone exposure with IgG/vehicle treatment and, were not significantly increased after etanercept treatment (Figure 3B). However, in *Notch3*$^{-/-}$ mice etanercept significantly reduced neutrophils compared to IgG controls ($P = 0.042$), but had no effect on neutrophil influx in *Notch4*$^{-/-}$ even though *Tnf* gene expression was increased in these mice (Figure 3B). Our results therefore support a TNF-α-mediated role for Notch3 but not Notch4 in protection against ozone-induced inflammation, and suggest the mechanism behind increased susceptibility is different for mice with targeted deletion of *Notch3* and *Notch4*. The link between TNF-α and Notch signaling likely occurs through NF-κB in a cell type and Notch receptor specific manner. Positive and negative regulation of NF-κB by Notch receptors has been demonstrated. For example, Notch1 and Notch2 negatively regulate Toll-like receptor (TLR) signaling in macrophages by inhibiting NF-κB transcription activity (Zhang et al. 2012). In contrast, Notch1 signaling activates NF-κB by suppressing an inhibitor of IκB kinase in T-cell acute lymphoblastic leukemia cells (Espinosa et al. 2010). TNF-α also regulates Notch signaling. In rheumatoid synovial fibroblasts, TNF-α stimulation induced expression of *Notch1* and *Notch4* and nuclear translocation of the intracellular domain (Ando et al. 2003). Additional investigations are necessary to understand the specific mechanistic interaction of TNF-α and Notch3 signaling in response to ozone.

Eosinophils were also significantly increased after ozone exposure, but only in *Notch3*$^{-/-}$ mice (Figure 1F). Currently there is no evidence that eosinophils express Notch3 receptors, but it has

been demonstrated both human and mouse eosinophils express Notch1 and Notch2 receptors that control eosinophil differentiation (Kang et al. 2007; Radke et al. 2009). In the present study the numbers of eosinophils counted after ozone exposure was very small, and although significant, it is unclear if the increase is biologically relevant. Eosinophils are known to cluster around airway nerves following ozone exposure so it possible that eosinophils are recruited to the lung by ozone but the majority remain in the tissue and do not migrate to the alveoli (Yost et al. 2005). Further investigation will be required to test this hypothesis.

Transcriptomic analysis identified candidate gene networks for Notch-mediated lung inflammation

Although TNF-α may influence a portion of Notch3-mediated protection against ozone-induced inflammation, additional mechanisms must contribute to the effect in mice with deletion of *Notch3* and *Notch4*. In order to further understand the downstream pathways through which *Notch3* and *Notch4* mediate ozone-induced lung inflammation, we used genome-wide transcriptome analysis to identify candidate gene transcripts and interactomes. ANOVA modeling of the data identified few differentially expressed genes between WT and knockout mice after air exposure (Supplemental Material, Table S2). However, ANOVA and pattern recognition EPIG [Extracting microarray gene expression Patterns and Identifying co-expressed Genes (Chou et al. 2007)] analyses identified ozone-induced changes in many gene transcripts in all genotypes (Figure 4A-C; Supplemental Material, Tables S2, S3, and S4).

To identify differential gene expression after ozone, transcripts were normalized to air exposure within each genotype. In WT and *Notch4*$^{-/-}$ mice, ANOVA modeling found the majority of differentially expressed gene transcripts were found after 24-48 hours ozone (Figure 4D). Across all time points, the greatest number of ozone responsive transcripts was found in *Notch3*$^{-/-}$ mice

(Figure 4D). Relative to WT, 7 biological function categories identified by Ingenuity Pathway Analysis (IPA) were similar in *Notch4*$^{-/-}$ mice and 3 (cellular growth and proliferation; cellular function and maintenance; hypersensitivity response) were unique to *Notch4*$^{-/-}$ (Figure 4E; Supplemental Material, Table S3). The biological function categories in *Notch3*$^{-/-}$ mice diverged from WT and *Notch4*$^{-/-}$. While 6 categories were in common with WT and *Notch3*$^{-/-}$, 3 categories (DNA replication, recombination, and repair; cellular assembly and organization; hepatic system disease) were unique to *Notch3*$^{-/-}$ mice (Figure 4E; Supplemental Material, Table S3). Although the inflammatory cell phenotypes of *Notch3*$^{-/-}$ and *Notch4*$^{-/-}$ mice were nearly identical, the greater number of differentially expressed transcripts in each biological function, and the greater diversity of transcripts in *Notch3*$^{-/-}$ mice are consistent with the hypothesis that mechanisms for protective effects of *Notch3* against ozone-induced inflammation differ from *Notch4*.

EPIG was used to further understand the expression patterns that underlie the mechanistically different protective effects of *Notch3* and *Notch4*. After normalization to respective air exposed controls, EPIG identified in WT, *Notch3*$^{-/-}$, and *Notch4*$^{-/-}$ mice 19 distinct patterns of gene expression with 1723 co-expressed transcripts (Figure 5A; Supplemental Material, Figure S1). The number of transcripts in each pattern ranged from 12 (pattern 19) to 281 (pattern 16) (Supplemental Material, Table S4).

We prioritized further analysis of three transcript patterns to profile ozone responsive transcripts common to all three genotypes (pattern 3), or unique to *Notch3* and *Notch4* (patterns 19 and 8) (Figure 5B, 5C, and 5D). Pattern 3 consisted of transcripts that increased after 24 and 48 hour ozone in all mice (Figure 5B; Supplemental Material, Table S4). The top significant gene ontology (GO) enrichment categories of these ozone-responsive genes included G protein-coupled receptor binding, chemokine and cytokine activity, and chemokine receptor binding

(Supplemental Material, Table S4). Included in pattern 3 are genes known to be associated with ozone-induced inflammation such as *Socs3* (Backus et al. 2010), *Myd88* (Bauer et al. 2011), and *Cxcl1* (Lazaar et al. 2011).

Pattern 19 profiles transcripts that decreased after 6 hours ozone only in *Notch3*$^{-/-}$ mice (Figure 5C). These *Notch3*$^{-/-}$ specific transcripts included tripartite motif containing genes (Trim) *Trim30*, *Trim12a*, *Trim5*, and *Trim6-Trim34*. Trim30 was recently described as a negative regulator of the inflammasome (Hu et al. 2010), a protein complex important for release of mature inflammatory cytokines IL-1β and IL-18 that is activated by a number of stimuli, including oxidant stress. Ozone causes oxidative stress and Feng et al. recently showed targeted deletion of various inflammasome components protects against ozone-induced lung inflammation (Feng et al. 2012). Thus, decreased expression of *Trim30* specifically in *Notch3*$^{-/-}$ mice may lead to increased inflammasome activation and enhanced ozone-induced lung inflammation.

Pattern 8 consisted of transcripts that increased after ozone exposure at all time points in *Notch4*$^{-/-}$ mice only (Figure 5D). These transcripts are significantly enriched for GO category positive regulation of immune system processes (Supplemental Material, Table S4); half of the identified genes in pattern 8 are expressed by at least one type of inflammatory cell and nine genes are expressed by stem cells (www.biogps.org). Transcripts included TNF receptor-associated factor 6 (*Traf6*), which is a unique member of the TNF receptor associated factor family that signals through the IL-1 receptor and TLR superfamily and is not activated by the TNF receptor. Activation of TRAF6 induces NF-κB through IκB kinase (Deng et al. 2000). Increased expression of *Traf6* in *Notch4*$^{-/-}$ mice may explain the increase in NF-κB activation seen in these mice 48 hours after ozone exposure (Figure 1J). The role of TRAF6 in ozone-induced lung

inflammation has not been identified, however IL-1 and TLR receptors are known to be important. Therefore, *Notch4* deficiency may enhance ozone-induced inflammation by increasing *Traf6* expression, thereby increasing activation of NF-κB and the inflammatory sequelae.

Notch receptors and their ligands are known to induce differentiation of T cell subsets (Amsen et al. 2004). Our gene expression analyses indicate that the absence of *Notch3* or *Notch4* caused differentially expressed genes involved in T cell signaling. In *Notch4* deleted mice after ozone exposure *Zap70* is upregulated (Supplemental Material, Table S4). Zap70 is part of the T cell receptor and is crucial for TCR signaling and development of CD8+ cells (Schim van der Loeff et al. 2014). In *Notch3* deleted mice, the ANOVA analysis indicated *Il33* is upregulated after 24 hours of ozone, which is an inducer of Th2 cytokines (Supplemental Material, Table S2). Therefore it is possible absence of Notch3 or Notch4 signaling affects T cell differentiation or development. Future studies will be necessary to characterize specific T cell populations present before and after ozone exposure in mice with *Notch3* and *Notch4* deletion.

Conclusion

In summary, we tested the hypothesis that *Inf2* cluster genes *Notch3* and *Notch4* contribute to ozone-induced lung inflammation. Enhanced inflammation in *Notch3*$^{-/-}$ and *Notch4*$^{-/-}$ mice relative to WT mice supports a novel role for Notch 3 and 4 receptors in modulating innate immune lung inflammatory responses to ozone. Moreover, genome-wide transcriptomic analyses suggest these receptors protect against inflammation through different mechanisms. Future investigations should provide greater insight to the role of innate immunity in differential susceptibility to oxidant injury.

References

Al-Hegelan M, Tighe RM, Castillo C, Hollingsworth JW. 2011. Ambient ozone and pulmonary innate immunity. Immunol Res 49:173-191.

Alexeeff SE, Litonjua AA, Wright RO, Baccarelli A, Suh H, Sparrow D, et al. 2008. Ozone exposure, antioxidant genes, and lung function in an elderly cohort: Va normative aging study. Occup Environ Med 65:736-742.

Amsen D, Blander JM, Lee GR, Tanigaki K, Honjo T, Flavell RA. 2004. Instruction of distinct cd4 t helper cell fates by different notch ligands on antigen-presenting cells. Cell 117:515-526.

Ando K, Kanazawa S, Tetsuka T, Ohta S, Jiang X, Tada T, et al. 2003. Induction of notch signaling by tumor necrosis factor in rheumatoid synovial fibroblasts. Oncogene 22:7796-7803.

Backus GS, Howden R, Fostel J, Bauer AK, Cho HY, Marzec J, et al. 2010. Protective role of interleukin-10 in ozone-induced pulmonary inflammation. Environ Health Perspect 118:1721-1727.

Bauer AK, Kleeberger SR. 2010. Genetic mechanisms of susceptibility to ozone-induced lung disease. Ann N Y Acad Sci 1203:113-119.

Bauer AK, Travis EL, Malhotra SS, Rondini EA, Walker C, Cho HY, et al. 2010. Identification of novel susceptibility genes in ozone-induced inflammation in mice. Eur Respir J 36:428-437.

Bauer AK, Rondini EA, Hummel KA, Degraff LM, Walker C, Jedlicka AE, et al. 2011. Identification of candidate genes downstream of tlr4 signaling after ozone exposure in mice: A role for heat-shock protein 70. Environ Health Perspect 119:1091-1097.

Bell ML, McDermott A, Zeger SL, Samet JM, Dominici F. 2004. Ozone and short-term mortality in 95 us urban communities, 1987-2000. JAMA 292:2372-2378.

Budinger GR, McKell JL, Urich D, Foiles N, Weiss I, Chiarella SE, et al. 2011. Particulate matter-induced lung inflammation increases systemic levels of pai-1 and activates coagulation through distinct mechanisms. PLoS One 6:e18525.

Chen C, Arjomandi M, Tager IB, Holland N, Balmes JR. 2007. Effects of antioxidant enzyme polymorphisms on ozone-induced lung function changes. Eur Respir J 30:677-683.

Cho HY, Zhang LY, Kleeberger SR. 2001. Ozone-induced lung inflammation and hyperreactivity are mediated via tumor necrosis factor-alpha receptors. Am J Physiol Lung Cell Mol Physiol 280:L537-546.

Cho HY, Morgan DL, Bauer AK, Kleeberger SR. 2007. Signal transduction pathways of tumor necrosis factor--mediated lung injury induced by ozone in mice. Am J Respir Crit Care Med 175:829-839.

Chou JW, Zhou T, Kaufmann WK, Paules RS, Bushel PR. 2007. Extracting gene expression patterns and identifying co-expressed genes from microarray data reveals biologically responsive processes. BMC Bioinformatics 8:427.

Deng L, Wang C, Spencer E, Yang L, Braun A, You J, et al. 2000. Activation of the ikappab kinase complex by traf6 requires a dimeric ubiquitin-conjugating enzyme complex and a unique polyubiquitin chain. Cell 103:351-361.

Espinosa L, Cathelin S, D'Altri T, Trimarchi T, Statnikov A, Guiu J, et al. 2010. The notch/hes1 pathway sustains nf-kappab activation through cyld repression in t cell leukemia. Cancer Cell 18:268-281.

Feng F, Li Z, Potts-Kant EN, Wu Y, Foster WM, Williams KL, et al. 2012. Hyaluronan activation of the nlrp3 inflammasome contributes to the development of airway hyperresponsiveness. Environ Health Perspect 120:1692-1698.

Hamade AK, Misra V, Rabold R, Tankersley CG. 2010. Age-related changes in cardiac and respiratory adaptation to acute ozone and carbon black exposures: Interstrain variation in mice. Inhal Toxicol 22 Suppl 2:84-94.

Hollingsworth JW, Maruoka S, Li Z, Potts EN, Brass DM, Garantziotis S, et al. 2007. Ambient ozone primes pulmonary innate immunity in mice. J Immunol 179:4367-4375.

Hu Y, Mao K, Zeng Y, Chen S, Tao Z, Yang C, et al. 2010. Tripartite-motif protein 30 negatively regulates nlrp3 inflammasome activation by modulating reactive oxygen species production. J Immunol 185:7699-7705.

Johansson E, Wesselkamper SC, Shertzer HG, Leikauf GD, Dalton TP, Chen Y. 2010. Glutathione deficient c57bl/6j mice are not sensitized to ozone-induced lung injury. Biochem Biophys Res Commun 396:407-412.

Kang JH, Lee da H, Seo H, Park JS, Nam KH, Shin SY, et al. 2007. Regulation of functional phenotypes of cord blood derived eosinophils by gamma-secretase inhibitor. Am J Respir Cell Mol Biol 37:571-577.

Kang JH, Kim BS, Uhm TG, Lee SH, Lee GR, Park CS, et al. 2009. Gamma-secretase inhibitor reduces allergic pulmonary inflammation by modulating th1 and th2 responses. Am J Respir Crit Care Med 179:875-882.

Kasahara DI, Kim HY, Williams AS, Verbout NG, Tran J, Si H, et al. 2012. Pulmonary inflammation induced by subacute ozone is augmented in adiponectin-deficient mice: Role of il-17a. J Immunol 188:4558-4567.

Kleeberger SR, Levitt RC, Zhang LY, Longphre M, Harkema J, Jedlicka A, et al. 1997. Linkage analysis of susceptibility to ozone-induced lung inflammation in inbred mice. Nat Genet 17:475-478.

Lazaar AL, Sweeney LE, MacDonald AJ, Alexis NE, Chen C, Tal-Singer R. 2011. Sb-656933, a novel cxcr2 selective antagonist, inhibits ex vivo neutrophil activation and ozone-induced airway inflammation in humans. Br J of Clin Pharmacol 72:282-293.

Lee YL, McConnell R, Berhane K, Gilliland FD. 2009. Ambient ozone modifies the effect of tumor necrosis factor g-308a on bronchitic symptoms among children with asthma. Allergy 64:1342-1348.

McDonnell WF. 1991. Intersubject variability in human acute ozone responsiveness. Pharmacogenetics 1:110-113.

Oakes JL, O'Connor BP, Warg LA, Burton R, Hock A, Loader J, et al. 2013. Ozone enhances pulmonary innate immune response to a toll-like receptor-2 agonist. Am J Respir Cell Mol Biol 48:27-34.

Okamoto M, Takeda K, Lucas JJ, Joetham A, Yasutomo K, Gelfand EW. 2012. Low-dose lipopolysaccharide affects lung allergic responses by regulating jagged1 expression on antigen-pulsed dendritic cells. Int Arch Allergy Immunol 157:65-72.

Osborne BA, Minter LM. 2007. Notch signalling during peripheral t-cell activation and differentiation. Nat Rev Immunol 7:64-75.

Post LC, Ternet M, Hogan BL. 2000. Notch/delta expression in the developing mouse lung. Mech Dev 98:95-98.

Prows DR, Shertzer HG, Daly MJ, Sidman CL, Leikauf GD. 1997. Genetic analysis of ozone-induced acute lung injury in sensitive and resistant strains of mice. Nat Genet 17:471-474.

Radke AL, Reynolds LE, Melo RC, Dvorak AM, Weller PF, Spencer LA. 2009. Mature human eosinophils express functional notch ligands mediating eosinophil autocrine regulation. Blood 113:3092-3101.

Schim van der Loeff I, Hsu LY, Saini M, Weiss A, Seddon B. 2014. Zap70 is essential for long-term survival of naive cd8 t cells. J Immunol 193:2873-2880.

Shore SA, Schwartzman IN, Le Blanc B, Murthy GG, Doerschuk CM. 2001. Tumor necrosis factor receptor 2 contributes to ozone-induced airway hyperresponsiveness in mice. Am J Respir Crit Care Med 164:602-607.

Tatum AJ, Shapiro GG. 2005. The effects of outdoor air pollution and tobacco smoke on asthma. Immunol Allergy Clin North Am 25:15-30.

Vancza EM, Galdanes K, Gunnison A, Hatch G, Gordon T. 2009. Age, strain, and gender as factors for increased sensitivity of the mouse lung to inhaled ozone. Toxicol Sci 107:535-543.

Yang IA, Fong KM, Zimmerman PV, Holgate ST, Holloway JW. 2008. Genetic susceptibility to the respiratory effects of air pollution. Thorax 63:555-563.

Yost BL, Gleich GJ, Jacoby DB, Fryer AD. 2005. The changing role of eosinophils in long-term hyperreactivity following a single ozone exposure. Am J Physiol Lung Cell Mol Physiol 289:L627-635.

Zhang Q, Wang C, Liu Z, Liu X, Han C, Cao X, et al. 2012. Notch signal suppresses toll-like receptor-triggered inflammatory responses in macrophages by inhibiting extracellular signal-regulated kinase 1/2-mediated nuclear factor kappab activation. J Biol Chem 287:6208-6217.

Figure Legends

Figure 1. *Notch3*$^{-/-}$ and *Notch4*$^{-/-}$ mice are more susceptible to ozone-induced lung inflammation compared to wild type mice (WT). (A) Bronchoalveolar lavage fluid (BALF) protein concentration increased significantly after 72 hours ozone in all mice (black bars). Protein concentration increased earliest (24 hours, medium gray bars), and most significantly in *Notch4*$^{-/-}$ mice. (B) BALF total cells increased in WT mice after 48 hours (dark gray bar) and in *Notch3*$^{-/-}$ and *Notch4*$^{-/-}$ mice after 72 hours. (C) Neutrophils significantly increased in *Notch3*$^{-/-}$ and *Notch4*$^{-/-}$ mice after 24-72 hours compared to air and WT mice. (D and E) BAL macrophages and monocytes significantly increased in *Notch3*$^{-/-}$ and *Notch4*$^{-/-}$ mice after 72 hours. (F**)** BAL eosinophils only significantly increased in *Notch3*$^{-/-}$ mice. (G) BAL lymphocytes only significantly increased in WT mice after 24 hours. (H) Expression of *Tnf* in whole lung homogenates significantly increased in *Notch3*$^{-/-}$ and *Notch4*$^{-/-}$ mice after 24 hours. (I) Expression of *Cxcl2* in whole lung homogenates increased in all groups after 24 hours. n = 4-10 mice per group (exposed in 2-3 groups), *$P < 0.05$ compared to respective air controls, †$P < 0.05$ compared to WT at same time point, #$P < 0.05$ between *Notch3*$^{-/-}$ and *Notch4*$^{-/-}$ mice at the same time point, 2-way ANOVA with Bonferroni post-hoc tests. (J) p65 NF-κB activation was significantly increased after 48 hours ozone in *Notch4*$^{-/-}$ mice and when compared to wild type and *Notch3*$^{-/-}$ mice. *$P < 0.05$ compared to respective air control, †$P < 0.05$ compared to WT and *Notch3*$^{-/-}$ ozone, 2-way ANOVA with Holm-Sidak pairwise comparisons.

Figure 2. Real time PCR of whole lung homogenates for Notch receptors, ligands, and target genes. Expression of *Notch1* and *Notch2* decreased in *Notch3*$^{-/-}$ and *Notch4*$^{-/-}$ mice after 48 hours of ozone. n = 3-10 mice per group (exposed in 2-3 groups), *$P < 0.05$ compared to respective air controls, 2-way ANOVA with Bonferroni post-hoc tests.

Figure 3. Blocking TNF signaling with etanercept reduced airway neutrophilia in *Notch3* knockout mice. Mice were treated prior to a 24-hour ozone exposure with a TNF inhibitor (etanercept, 10 mg/kg i.p.) or vehicle (human IgG, 10 mg/kg i.p.). (A) Etanercept pre-treatment did not affect BALF protein concentration. (B) Etanercept reduced the ozone-induced influx of neutrophils in *Notch3*$^{-/-}$ mice. n = 5-10 mice per group, *$P < 0.05$ compared to respective air

controls, #$P < 0.05$ between etanercept and vehicle after ozone, 2-way ANOVA with Tukey's post-hoc tests.

Figure 4. Gene expression microarray from whole lung homogenates identified differentially expressed genes after ozone. (A) In wild type mice (WT) 116 transcripts were differentially expressed after ozone compared to air. (B) In *Notch3*$^{-/-}$ mice 739 transcripts were differentially expressed after ozone compared to air. (C) In *Notch4*$^{-/-}$ mice 155 differentially expressed transcripts after ozone compared to air. $P < 0.05$, ANOVA with Tukey's HSD post-hoc test and Benjamini-Hochberg multiple testing correction. (D) Number of differentially expressed genes after ozone compared to air. (E) Top 10 significant biological functions from Ingenuity Pathway Analysis and numbers of differentially expressed genes in each category.

Figure 5. Pattern analysis of transcript expression using EPIG (Extracting microarray gene expression Patterns and Identifying co-expressed Genes) identified candidate genes. (A) Heat map of 1723 transcripts that fit in 19 patterns (labeled numerically) identified by EPIG (see Supplemental Material, Table S4 for full list of genes in all patterns). Red and blue colors correspond to up and down regulated, respectively. Transcripts are colored by fold change relative to respective air controls. (B) Pattern 3 represents transcripts that increased after 24 (triangles) and 48 (squares) hours ozone in all genotypes (232 transcripts, top 14 most significant are shown). (C) Pattern 19 represents transcripts that decrease after 6 hours (circles) ozone only in *Notch3*$^{-/-}$ mice (12 transcripts, top 9 shown). (D) Pattern 8 represents transcripts that change only in *Notch4*$^{-/-}$ mice. These transcripts increase after ozone at all time points (50 transcripts, top 11 shown). Profiles in (B), (C) and (D) represent the average of the top 6 gene probeset profiles within the respective pattern. The vertical axes are the changes in gene expression (log2 intensity) relative to air-exposed controls.

Figure 1

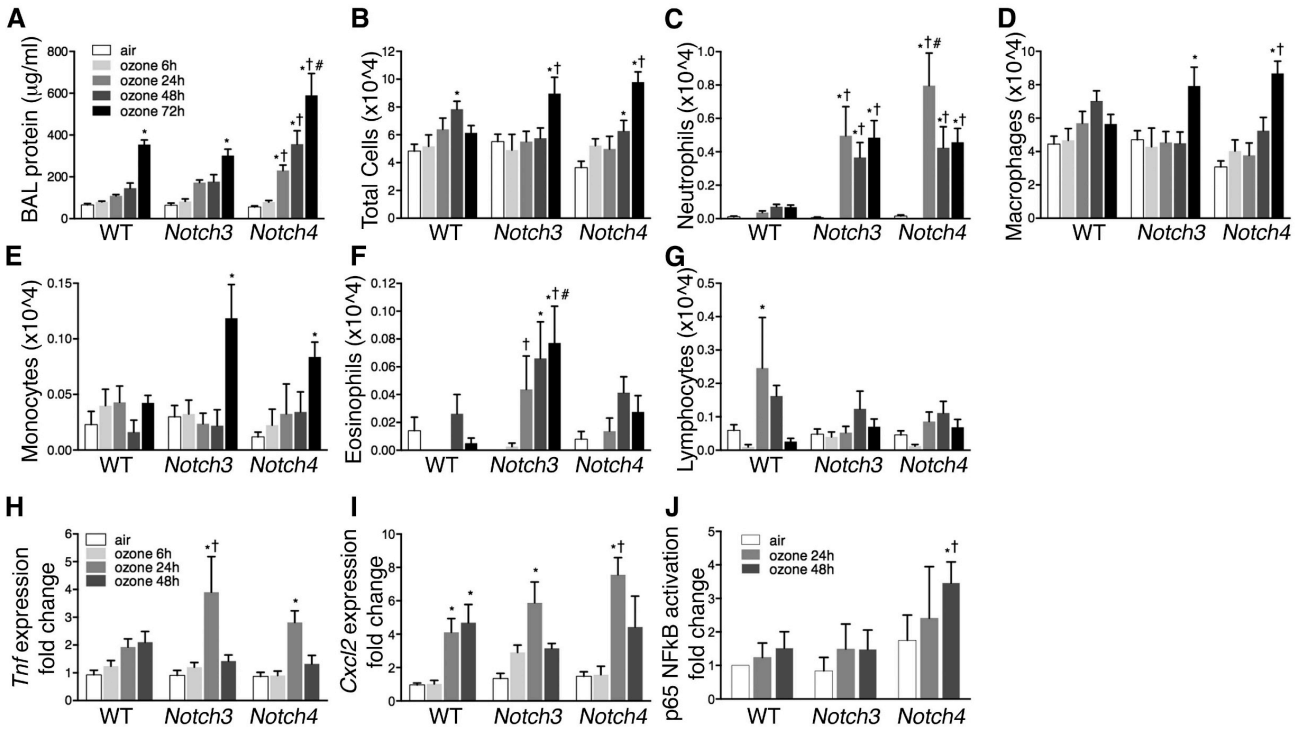
A
BAL protein (µg/ml)
air
ozone 6h
ozone 24h
ozone 48h
ozone 72h
WT
Notch3
Notch4
B
Total Cells (x10^4)
C
Neutrophils (x10^4)
D
Macrophages (x10^4)
E
Monocytes (x10^4)
F
Eosinophils (x10^4)
G
Lymphocytes (x10^4)
H
Tnf expression fold change
I
Cxcl2 expression fold change
J
p65 NFkB activation fold change
ozone 24h
ozone 48h

Figure 2

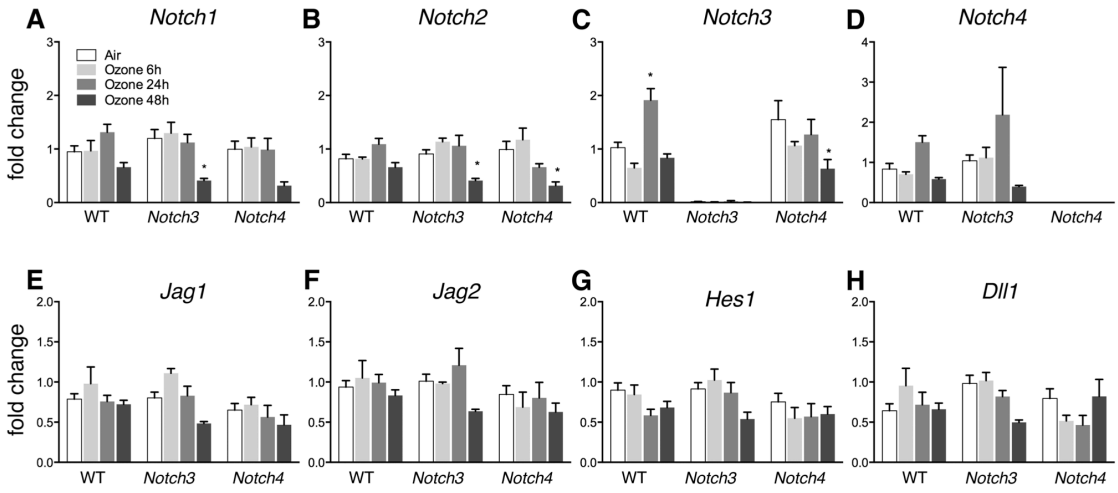
A
Notch1
B
Notch2
C
Notch3
D
Notch4
Air
Ozone 6h
Ozone 24h
Ozone 48h
fold change
WT
Notch3
Notch4
E
Jag1
F
Jag2
G
Hes1
H
Dll1

Figure 3

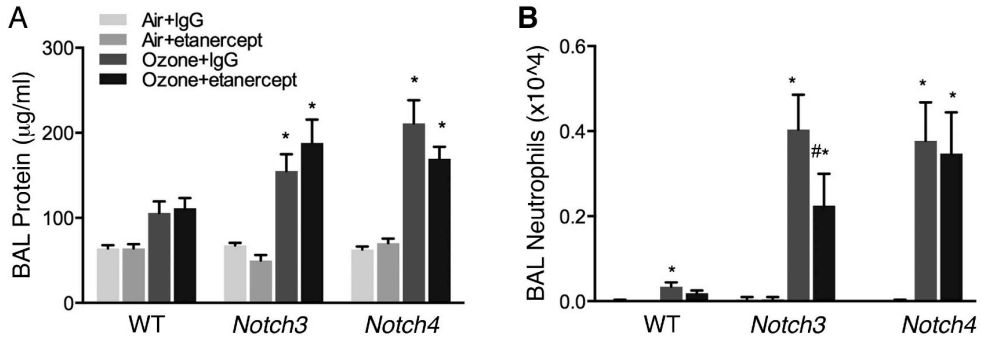
A
Air+IgG
Air+etanercept
Ozone+IgG
Ozone+etanercept
BAL Protein (μg/ml)
300
200
100
0
WT
Notch3
Notch4
B
BAL Neutrophils (x10^4)
0.6
0.4
0.2
0.0
#*
WT
Notch3
Notch4

Figure 4

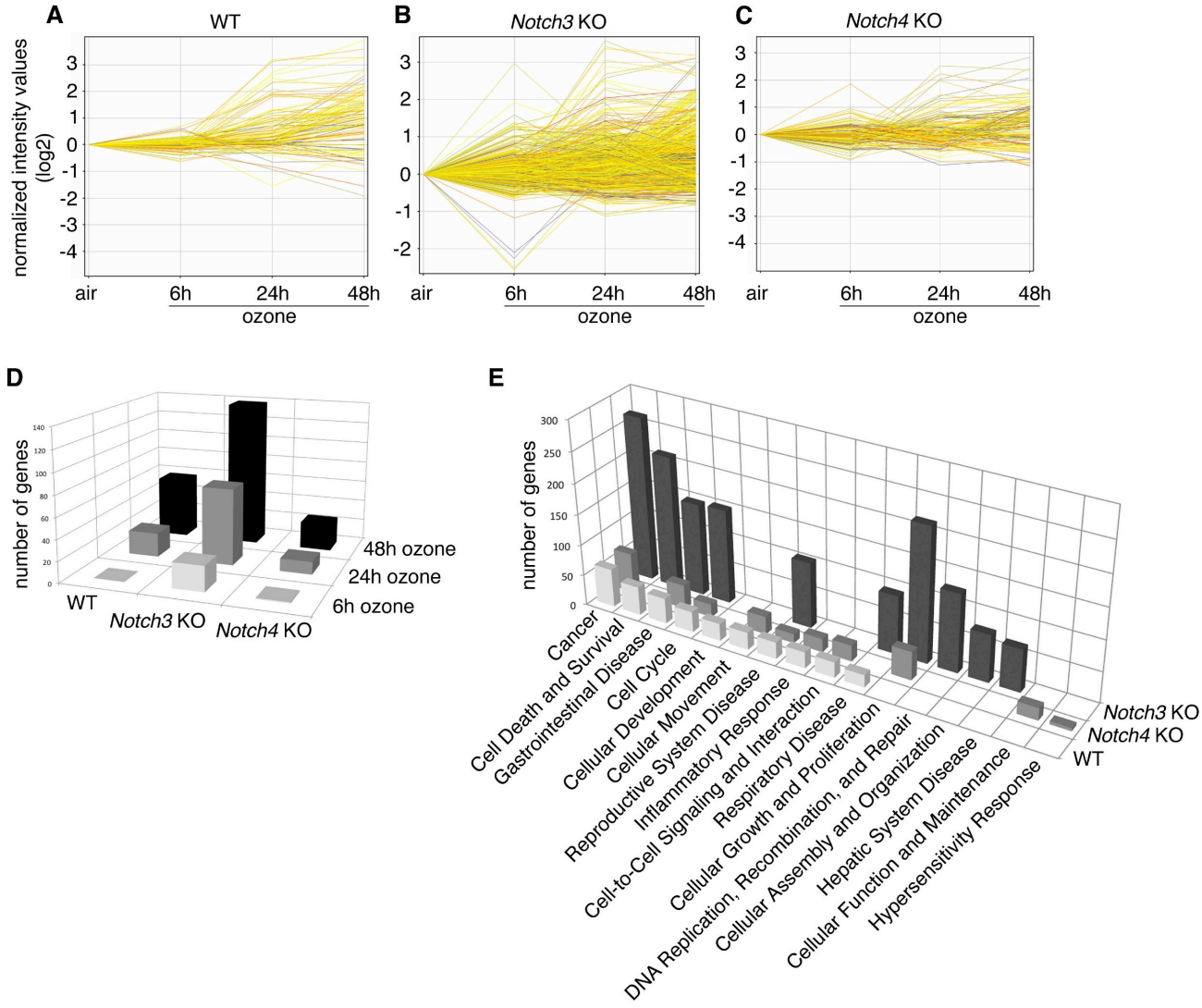
A
WT
B
Notch3 KO
C
Notch4 KO
normalized intensity values (log2)
air
6h
24h
48h
ozone
D
number of genes
48h ozone
24h ozone
6h ozone
WT
Notch3 KO
Notch4 KO
E
number of genes
Cancer
Cell Death and Survival
Gastrointestinal Disease
Cell Cycle
Cellular Development
Cellular Movement
Reproductive System Disease
Inflammatory Response
Cell-to-Cell Signaling and Interaction
Respiratory Disease
Cellular Growth and Proliferation
DNA Replication, Recombination, and Repair
Cellular Assembly and Organization
Hepatic System Disease
Cellular Function and Maintenance
Hypersensitivity Response
Notch3 KO
Notch4 KO
WT

Figure 5

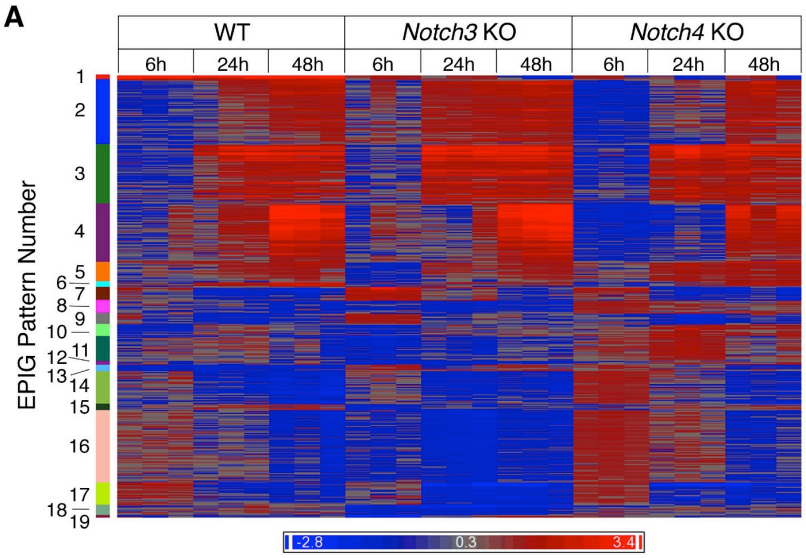

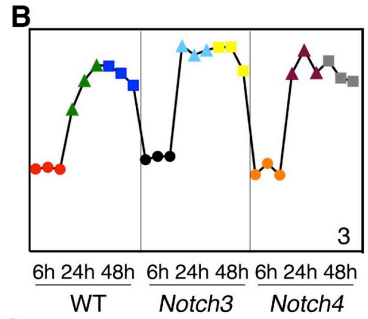

Affy ID	Symbol	Title
1449133_at	*Sprr1a*	small proline-rich protein 1A
1460227_at	*Timp1*	tissue inhibitor of metalloproteinase 1
1419431_at	*Ereg*	epiregulin
1419413_at	*Ccl17*	chemokine (C-C motif) ligand 17
1416592_at	*Glrx*	glutaredoxin
1416576_at	*Socs3*	suppressor of cytokine signaling 3
1450826_a_at	*Saa2*	serum amyloid A2
1451416_a_at	*Tgm1*	transglutaminase 1, K polypeptide
1420352_at	*Prss22*	protease, serine, 22
1438148_at	*Cxcl1*	chemokine (C-X-C motif) ligand 1 (KC)
1449015_at	*Retnla*	resistin like alpha
1416563_at	*CTPS1*	cytidine 5'-triphosphate synthase
1439878_at	*Ivl*	involucrin
1419272_at	*Myd88*	myeloid differentiation primary response gene 88

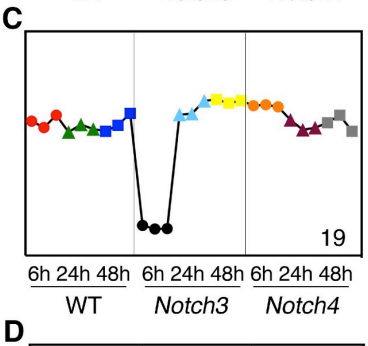

Affy ID	Symbol	Title
1435665_at	*Trim30d*	tripartite motif-containing 30D
1437432_a_at	*Trim12a*	tripartite motif-containing 12A
1424857_a_at	*Trim34*	tripartite motif-containing 34A
1436061_at	*Chaf1a*	chromatin assembly factor 1, subunit A (p150)
1442693_at	*Trim5*	tripartite motif-containing 5
1426633_s_at	*Kctd14*	potassium channel tetramerisation domain containing 14
1418239_at	*Apof*	apolipoprotein F
1421385_a_at	*Myo7a*	myosin VIIA
1426334_a_at	*Bcl2l11*	BCL2-like 11 (apoptosis facilitator)

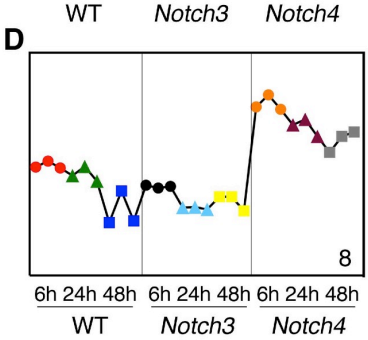

Affy ID	Symbol	Title
1439899_at	*Galnt13*	UDP-N-acetyl-alpha-D-galactosamine:polypeptide N-acetylgalactosaminyltransferase 13
1434816_at	*Vps33a*	vacuolar protein sorting 33 homolog A (S. cerevisiae)
1448028_at	*Tbc1d24*	TBC1 domain family, member 24
1448405_a_at	*Eid1*	EP300 interacting inhibitor of differentiation 1
1420444_at	*Slc22a3*	solute carrier family 22 (organic cation transporter), member 3
1436098_at	*Bche*	butyrylcholinesterase
1428759_s_at	*Cwc25*	CWC25 spliceosome-associated protein homolog (S. cerevisiae)
1458820_at	*Znf778*	zinc finger protein 778
1450664_at	*Gabpa*	GA repeat binding protein, alpha
1439632_at	*Gnb4*	guanine nucleotide binding protein (G protein), beta 4
1446977_at	*Traf6*	TNF receptor-associated factor 6